21 June 2023

Masses and springs - a toy model coming to life

Richard Craster Department of Mathematics, Imperial College London

- The toy in 2D and 3D
- Maxwell's equations - homogenisation and numerics
- Asymptotic theories for close spacing
- Topological models
- Box crystals
- Experiments in 3D

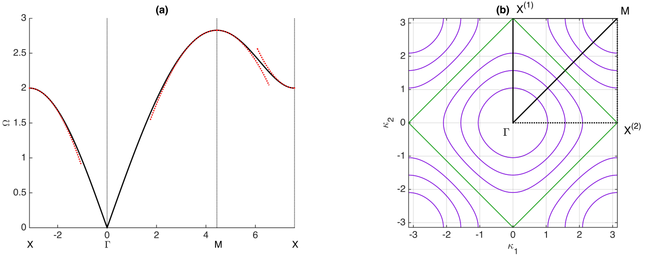

$$y_{n+1,m} + y_{n-1,m} + y_{n,m+1} + y_{n,m-1} + (\Omega^2 - 4)y_{n,m} = \delta_{0,0}$$

$$y_{n,m} = \frac{1}{(2\pi)^2} \int_{-\pi}^{\pi} \int_{-\pi}^{\pi} \frac{\exp[-i(k_1 n + k_2 m)]}{D(\Omega, k_1, k_2)} \mathrm{d}k_1 \mathrm{d}k_2.$$

Dropping the forcing and setting $y_{n+N,m+M} = \exp(i[\kappa_1 N + \kappa_2 M])y_{n,m}$ givrs

$$D(\Omega, \kappa_1, \kappa_2) = \Omega^2 - 4 + 2(\cos\kappa_1 + \cos\kappa_2) = 0.$$

Elliptic near M

Standing wave frequency is $\Omega_0 = \sqrt{8}$

$$\Omega^2 \sim \Omega_0^2 + \epsilon^2 \Omega_2^2$$

In the integral $k_1 = \pi + \epsilon\alpha$, $k_2 = \pi + \epsilon\beta$, using the periodicity of the integral and thereby centring the region of integration at M.

$$y_{n,m} = \frac{\exp[-i\pi(n+m)]}{(2\pi)^2} \int_{-\infty}^{\infty}\int_{-\infty}^{\infty} \frac{\exp[-i(\alpha\eta_1 + \beta\eta_2)]}{\alpha^2 + \beta^2 + \Omega_2^2} \mathrm{d}\alpha \mathrm{d}\beta + \mathcal{O}(\epsilon),$$

Use long-scale variable $\eta = (\eta_1, \eta_2) = \epsilon(n, m)$.
Short-scale oscillatory piece $Y_{n,m} = \exp[-i(n+m)\pi]$, and a long-scale component $f(\eta)$ so $y_{n,m} = Y_{n,m} f(\eta) + O(\epsilon)$.

$$f(\eta) = \begin{cases} \frac{1}{2\pi} K_0\left(\sqrt{\Omega_2^2} r\right) & \text{if} \quad \Omega_2^2 > 0 \\ \frac{i}{4} H_0^{(1)}\left(\sqrt{-\Omega_2^2} r\right) & \text{if} \quad \Omega_2^2 < 0 \end{cases},$$

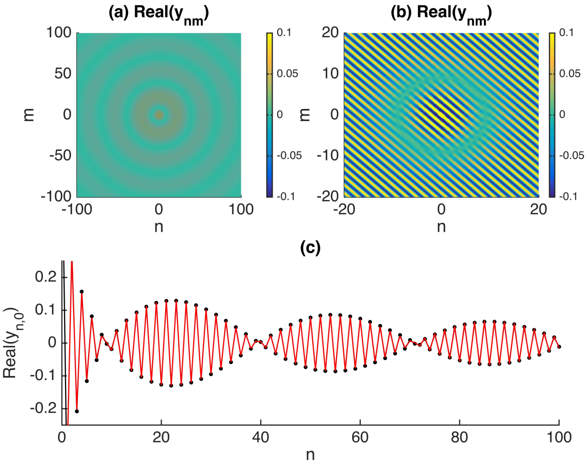

$\Omega = \sqrt{8 - 0.01}$, incidentally from HFH

$$f_{\eta_1\eta_1}(\eta) + f_{\eta_2\eta_2}(\eta) - \Omega_2^2 f(\eta) = -\delta(\eta_1)\delta(\eta_2)$$

Near X

The wavenumber at X $(= X^{(1)})$ has, from the symmetries of the irreducible Brillouin zone, a related point $X^{(2)}$ at $(\pi, 0)$ and the standing wave frequency is $\Omega_0 = 2$. Set $k_1 = \epsilon\alpha$, $k_2 = \pi + \epsilon\beta$

$$y_{n,m} = \frac{\exp[-im\pi]}{(2\pi)^2} \int_{-\infty}^{\infty} \int_{-\infty}^{\infty} \frac{\exp[-i(\alpha\eta_1 + \beta\eta_2)]}{-\alpha^2 + \beta^2 + \Omega_2^2} \mathrm{d}\alpha \mathrm{d}\beta + \mathcal{O}(\epsilon),$$

Short-scale an oscillatory component $Y_{n,m} = \exp[-im\pi]$ and on the long-scale an integral, which has solution

$$f(\eta) = \begin{cases} AH_0^{(1)}\left(\sqrt{\rho^2\Omega_2^2}\right) & \text{if} \quad \rho^2\Omega_2^2 > 0 \\ BK_0\left(\sqrt{-\rho^2\Omega_2^2}\right) & \text{if} \quad \rho^2\Omega_2^2 < 0 \end{cases},$$

where $\rho^2 = \eta_1^2 - \eta_2^2$, A and B are constants, $H_0^{(1)}$ is the Hankel function and K_0 the modified Bessel function. There is a logarithmic singularity where $\eta_1 = \pm\eta_2$, on the diagonals, hence the solution is divided into pieces valid in different quadrants

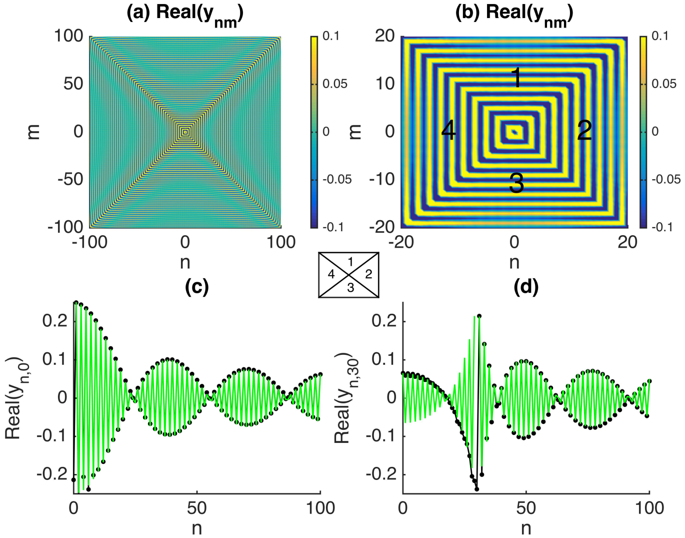

The field excited by a source at frequency $\Omega = \sqrt{4 - 0.01}$ at point X of the Brillouin zone

Three dimensions

$$y_{m+1,n,p} + y_{m-1,n,p} + y_{m,n+1,p} + y_{m,n-1,p} + y_{m,n,p+1} + y_{m,n,p-1}$$

$+(\Omega^2 - 6)y_{m,n,p} = \delta_{0,0,0}$
The dispersion relation relating $\kappa = (\kappa_1, \kappa_2, \kappa_3)$ to frequency Ω, in the absence of forcing, is

$$D(\Omega, \kappa_1, \kappa_2, \kappa_3) = \Omega^2 - 6 + 2(\cos\kappa_1 + \cos\kappa_2 + \cos\kappa_3) = 0,$$

Fourier solution

$$y_{m,n,p} = \frac{1}{(2\pi)^3} \int_{-\pi}^{\pi} \int_{-\pi}^{\pi} \int_{-\pi}^{\pi} \frac{\exp[-i(k_1 m + k_2 n + k_3 p)]}{D(\Omega, k_1, k_2, k_3)} \mathrm{d}k_1 \mathrm{d}k_2 \mathrm{d}k_3$$

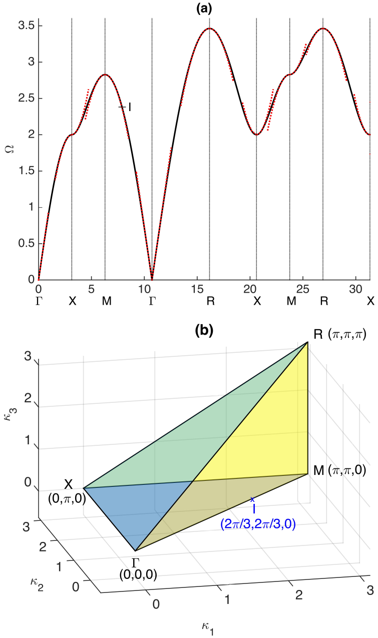
(a)
Ω
3.5
3
2.5
2
1.5
1
0.5
0
0 5 10 15 20 25 30
Γ X M Γ R X M R X
I
(b)
R (π,π,π)
M (π,π,0)
X
(0,π,0)
Γ
(0,0,0)
I
(2π/3,2π/3,0)
κ3
κ2
κ1

Near X

Wavevector has coordinates $(0, \pi, 0)$ and the standing wave frequency is $\Omega_0 = 2$. Make change of variables $k_1 = \epsilon\alpha$, $k_2 = \pi + \epsilon\beta$, $k_3 = \epsilon\gamma$, gives

$$y_{m,n,p} = \frac{e^{-in\pi}}{(2\pi)^3}\epsilon \int\limits_{-\infty}^{\infty}\int\limits_{-\infty}^{\infty}\int\limits_{-\infty}^{\infty} \frac{\exp[-i(\alpha\eta_1 + \beta\eta_2 + \gamma\eta_3)]}{-\alpha^2 + \beta^2 - \gamma^2 + \Omega_2^2} \mathrm{d}\alpha \mathrm{d}\beta \mathrm{d}\gamma + \mathcal{O}(\epsilon^2)$$

Long-scale variable is $\eta = (\eta_1, \eta_2, \eta_3) = \epsilon(m, n, p)$. $Y_{m,n,p} = \epsilon \exp[-in\pi]$ and a long-scale function

$$f(\eta) = \frac{\exp\left[i\sqrt{\Omega_2^2\rho^2}\right]}{4\pi\rho}, \qquad (0.1)$$

where $\rho^2 = \eta_1^2 - \eta_2^2 + \eta_3^2$;

$$f_{\eta_1\eta_1}(\eta) - f_{\eta_2\eta_2}(\eta) + f_{\eta_3\eta_3}(\eta) + \Omega_2^2 f(\eta) = \delta(\eta_1)\delta(\eta_2)\delta(\eta_3),$$

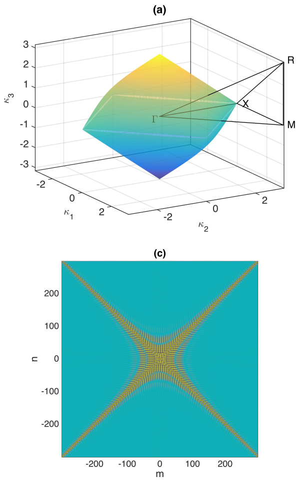

(a)
(b)
(c)
(d)
κ_1
κ_2
κ_3
R
X
M
Γ
m
n

Example from Maxwell's equation

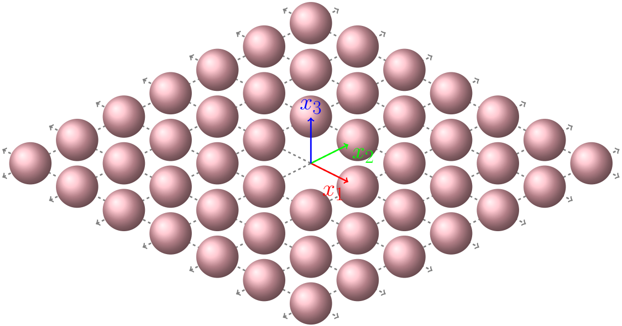

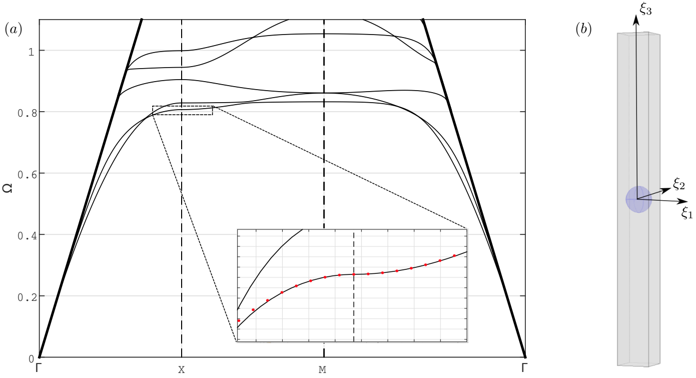

(a)
1
0.8
0.6
0.4
0.2
0
Ω
Γ
X
M
Γ
(b)
ξ_3
ξ_2
ξ_1

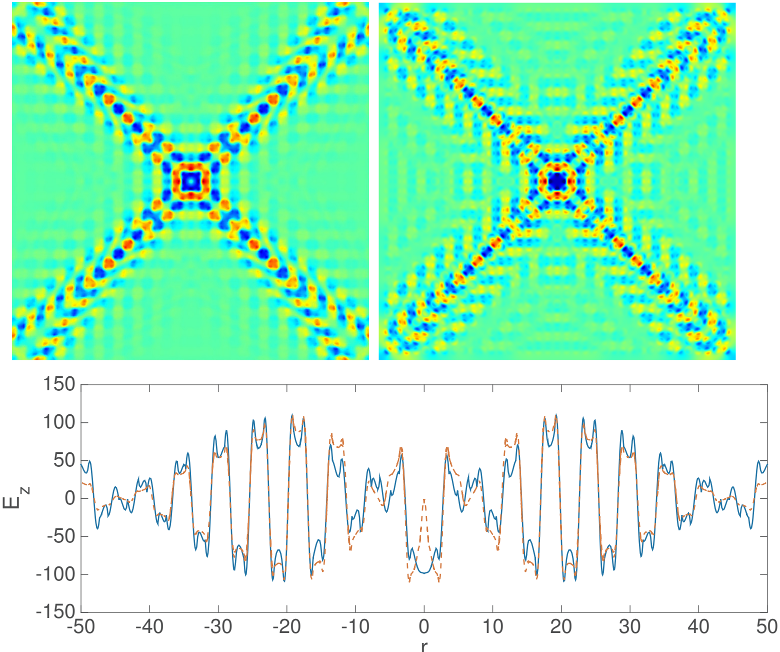
150
100
50
0
-50
-100
-150
E_z
-50
-40
-30
-20
-10
0
10
20
30
40
50
r

Asymptotics

- Many of the exciting results in topological wave physics have their origin in tight-binding models from quantum mechanics that are discrete networks.
- There is a strong demand for robust redirection of light/ em/ acoustic waves using topological ideas.
- Many empirical fitting methods for closely spaced objects with "lumped parameter models", there is an asymptotic model with no fitting.
- Many topological (discrete) systems protected by chiral symmetry, but this is broken by long-range interactions so not trivially achievable in continua - but here we achieve this.

Simple photonic/phononic crystal

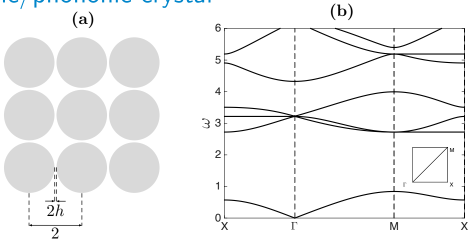

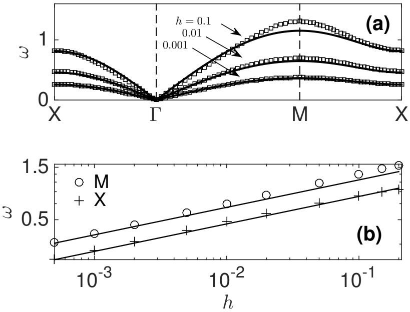

Asymptotic method - physics

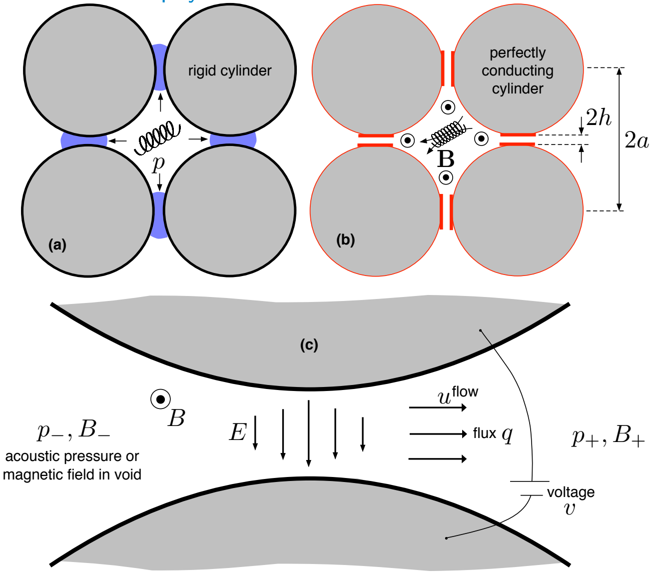

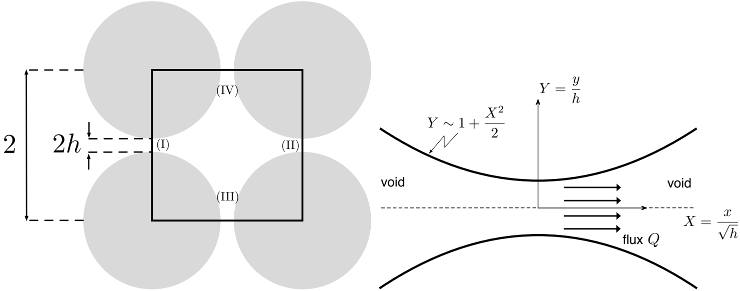

Inner problem takes the local curvatures (R_1, R_2) into account. Outer problem / matching connects the inner problems. The pressures in void n, m are the unknowns.

Result for a square lattice and cylinders of radius a

A discrete wave equation emerges as

$$\frac{A_0}{c^2\delta}\frac{d^2 p_{n,m}}{dt^2} = p_{n,m+1} + p_{n,m-1} + p_{n-1,m} + p_{n+1,m} - 4p_{n,m}, \qquad (1.2)$$

where $c^2 = \gamma p_0/\rho_0$ is the speed of sound squared.
δ is normalised acoustic conductivity

$$\delta = \frac{1}{\pi}\sqrt{\frac{2h}{a}} \ll 1. \qquad (1.3)$$

Much more general than just cylinders, or a square array. By varying the local curvatures, δ_{nm} or void A_{0nm} or lattice we now have a non-lumped parameter route back and forth discrete and continuous.

A. Vanel, O. Schnitzer , R. V. Craster, EPL, 119, 2017

Valley Hall

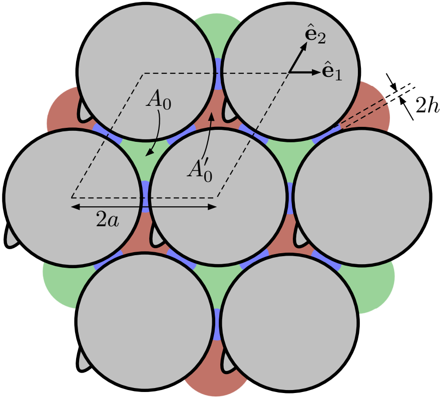

A closely packed hexagonal lattice of cylinders forms a honeycomb network of voids connected by narrow gaps. Inversion symmetry is broken by making the areas of the two voids in each unit cell different

$$\frac{A_0}{c^2\delta}\frac{\partial^2 p_{n,m}}{\partial t^2} = p'_{n,m} + p'_{n-1,m} + p'_{n,m-1} - 3p_{n,m}, \tag{1.4}$$

$$\frac{A'_0}{c^2\delta}\frac{\partial^2 p'_{n,m}}{\partial t^2} = p_{n,m} + p_{n+1,m} + p_{n,m+1} - 3p'_{n,m}, \tag{1.5}$$

where $p_{n,m}$ and $p'_{n,m}$ are the pressures in the two voids, respectively of areas A_0 and A'_0, within unit cell (n, m); the indexes n and m represent $2a$ displacements in the $\hat{\mathbf{e}}_1 = \hat{\mathbf{e}}_x$ and $\hat{\mathbf{e}}_2$ directions shown in Fig. **??**. The dispersion relation follows as

$$\frac{A_0 A'_0}{c^4\delta^2}\Omega^4 - \frac{3(A_0 + A'_0)}{c^2\delta}\Omega^2 + 6 - 2\cos(2\kappa_x a) - 4\cos(\kappa_x a)\cos(\sqrt{3}\kappa_y a) = 0. \tag{1.6}$$

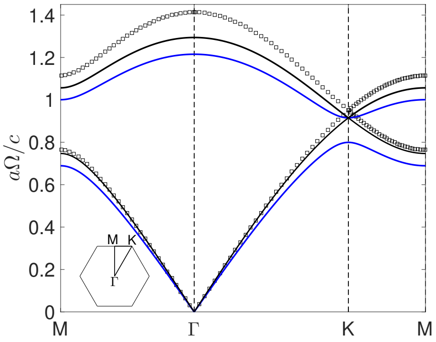

The acoustic branch for the hexagonal array of circular cylinders ($h/a = 0.01$, symbols are numerics and black line is (1.6) for $A_0 = A_0'$). Insertion of a defect opens the hexagon-lattice Dirac point at K (solid blue line is (1.6) for $A_0' - A_0 = 0.05a^2$).

Topological example

Wu and Hu PRL (2015) gave a remarkable example mimicking quantum spin hall in photonics. Dielectric honeycomb of inclusions with symmetry broken.

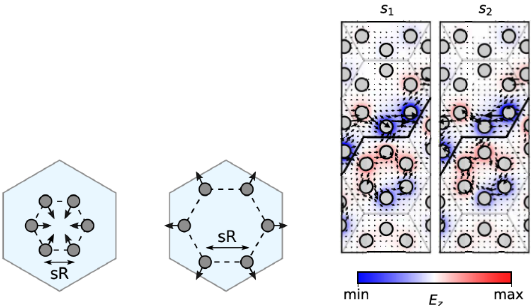

Figures taken from Plasmonic version by M. Proctor et al ACS Photonics 2019

Closely spaced version

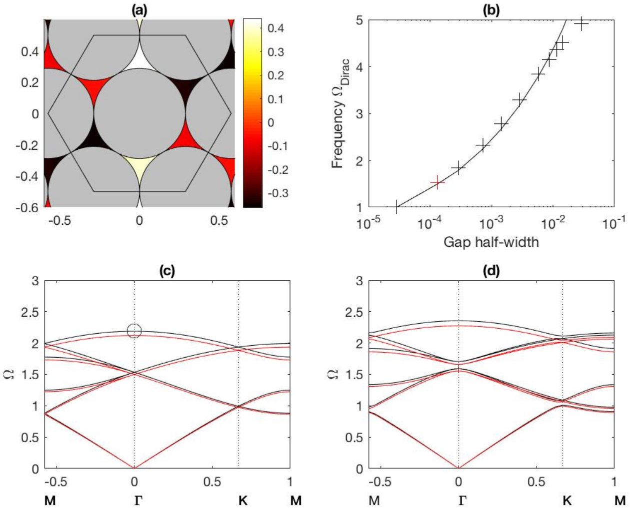

Kagome model

We will need the Kagome model later, so let us briefly describe it

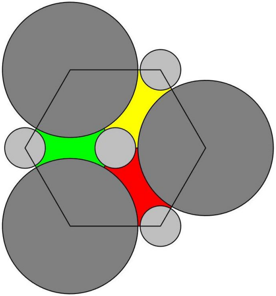

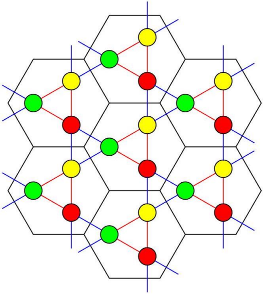

Kagome model

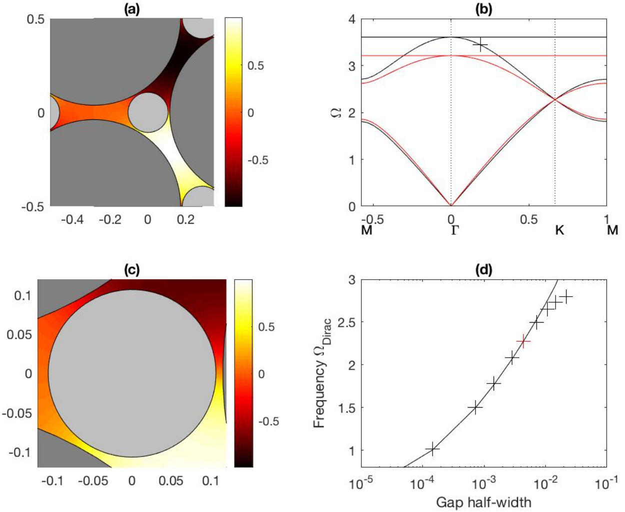

Note the flat band

Square-root semi-metal

Following, say, Mizoguchi et al PRB 2021. Let us look at a tight-binding model for the honeycomb-kagome model and its topological properties.

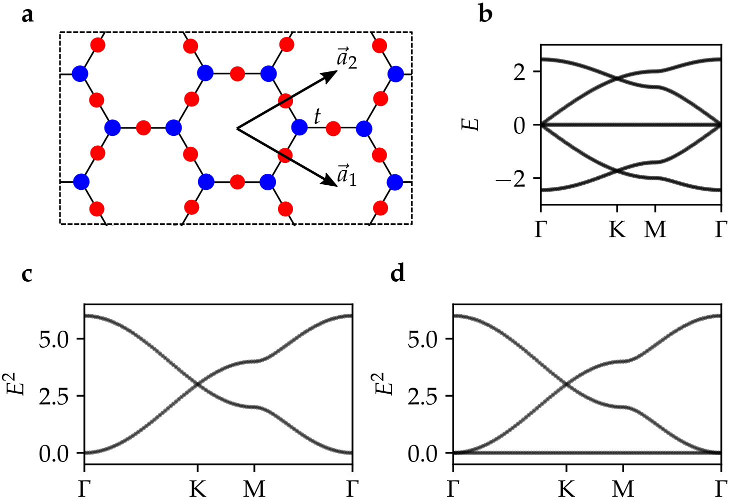

Tight-binding

The Hamiltonian has a block off-diagonal form,

$$H_{\vec{k}}^{\mathsf{hk}} \begin{bmatrix} u_1 \\ \vdots \\ u_5 \end{bmatrix} = \begin{bmatrix} 0_{2\times 2} & t\Psi_{\vec{k}}^{\dagger} \\ t\Psi_{\vec{k}} & 0_{3\times 3} \end{bmatrix} \begin{bmatrix} u_1 \\ \vdots \\ u_5 \end{bmatrix}, \qquad (1.7)$$

Hoppings between different sublattices and chiral symmetric.

$$\left(H_{\vec{k}}^{\mathsf{hk}}\right)^2 = \begin{bmatrix} t^2\Psi_{\vec{k}}^{\dagger}\Psi_{\vec{k}} & 0_{2\times 3} \\ 0_{3\times 2} & t^2\Psi_{\vec{k}}\Psi_{\vec{k}}^{\dagger} \end{bmatrix} = \begin{bmatrix} H_{\vec{k}}^{\mathrm{h}} & 0_{2\times 3} \\ 0_{3\times 2} & H_{\vec{k}}^{\mathrm{k}} \end{bmatrix}, \qquad (1.8)$$

A square-root Hamiltonian: Honeycomb Kagome is a square-root topological semi-metal with non-trivial topology.

The photonic version

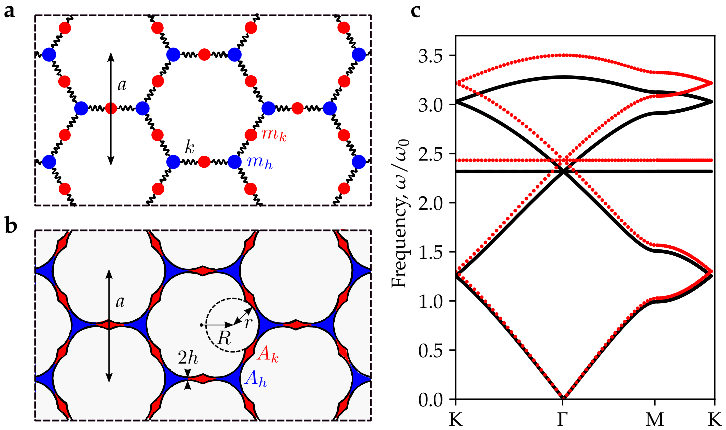

Palmer, Ignatov, Craster, Makwana, New J. Phys. 24, 053020, 2022

Edge states

We can now create topologically protected edge states using results from semi-metals.

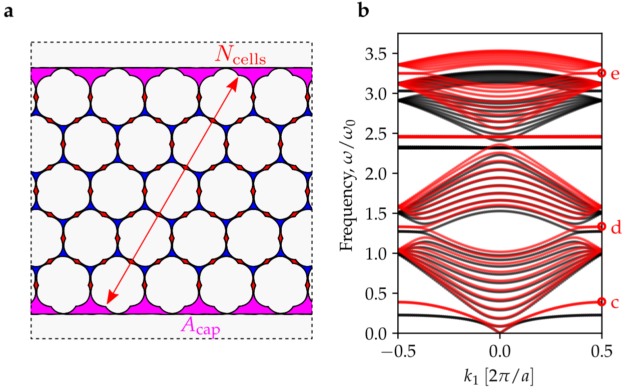

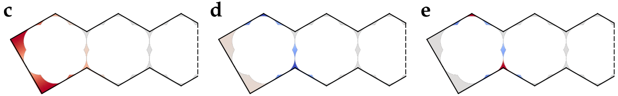

Finite structures - just discrete model